

Clara Lemos¹, Volker K. Schulze¹, Benjamin Bader¹, Clara D. Christ¹, Hans Briem¹, Oliver Politz¹, Florian Prinz¹, Simon Holton¹, Ulf Bömer¹, Tobias Heinrich¹, Julien Lefranc¹, Philip Lienau¹, Arne Scholz¹, Franz von Nussbaum², Carl Friedrich Nising¹, Dominik Mumberg¹, Marcus Bauser¹, Andrea Hägebarth¹

¹Bayer AG, Pharmaceutical Division, Berlin, Germany; ²Bayer S.A.S., Crop Science Division, Lyon, France

INTRODUCTION

- AMP-activated protein kinase (AMPK) is a sensor of the energy status in cells and it plays a key role in controlling cell metabolism.
- AMPK is a component of the liver kinase B1 (LKB1) tumor suppressor cascade, which inhibits mammalian target of rapamycin complex 1 (mTORC1) and has mainly been perceived as a tumor suppressor. However, in the last few years, studies have suggested that AMPK might actually exert a pro-tumorigenic role in certain contexts.^{1,2}
- MYC is a proto-oncogene upregulated in many forms of cancer. Dysregulated MYC expression has been demonstrated to render tumor cells sensitive to AMPK depletion. Due to their increased anabolism, MYC-dependent cells rely on AMPK to restore ATP levels and to prevent an energy crisis resulting in apoptosis and cell death (Fig. 1).³
- After target validation using siRNA, our aim was to develop potent and selective AMPK inhibitors to evaluate the therapeutic potential of inhibiting AMPK in MYC-driven tumors.

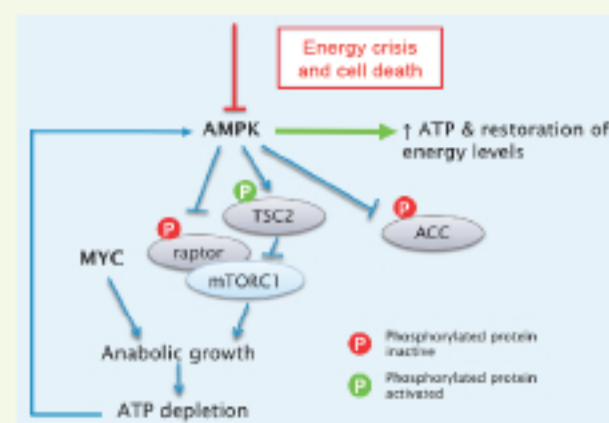


Figure 1. Target rationale for inhibiting AMPK in MYC-dependent cells. MYC dysregulation triggers increased anabolic activity, resulting in ATP depletion. As a result, AMPK is activated to reduce anabolic activities and to restore cellular energy levels via inactivation of mTORC1. In MYC-dependent cells, the inhibition of AMPK results in the activation of mTORC1 and subsequent anabolic effects, leading to an energy crisis and induction of apoptosis (scheme based on Liu et al. 2012).³ ACC, acetyl-CoA carboxylase; AMPK, 5' adenosine monophosphate-activated protein kinase; ATP, adenosine triphosphate; mTORC1, mammalian target of rapamycin complex 1; TSC2, tuberous sclerosis complex 2.

RESULTS

Structure-activity relationship (SAR) analysis of the high-throughput screening (HTS) hits and first analogues

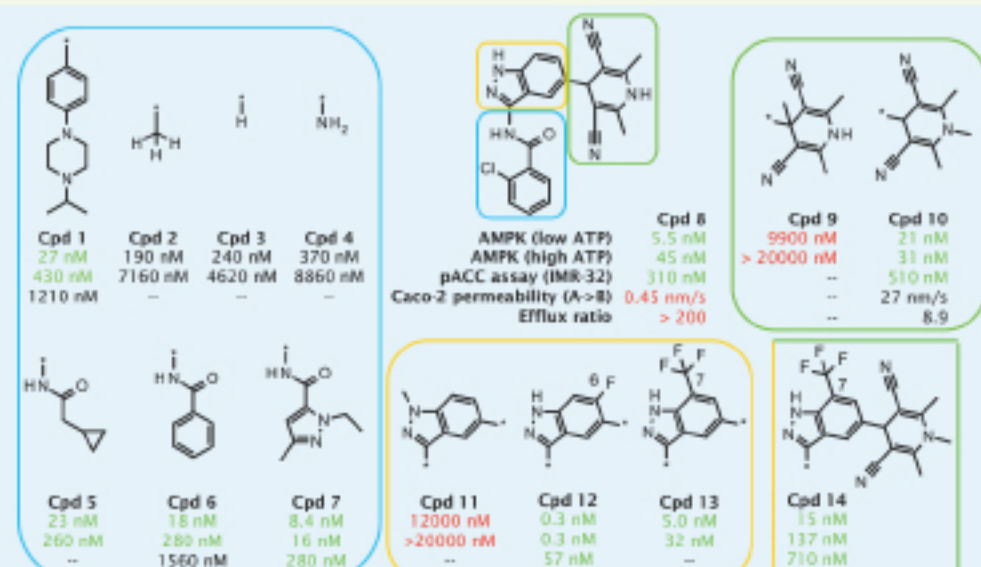


Figure 2. Structure-activity relationship (SAR) of high-throughput screening (HTS) hits and first analogues as determined by AMPK kinase, cellular mechanistic pACC, and Caco-2 permeability assays. Cpd, compound; pACC, phosphorylated acetyl-CoA carboxylase.

- Amides showed improved potency (blue box), in particular 2-chloro-benzamides (compounds 8 and 12) had very high potency (Fig. 2).
- The F-substituent at carbon 6 (C6) of the dihydropyridine (DHP) core improved potency (compound 12, yellow box).
- Compounds with N-Me substituted DHP generally had better Caco-2 permeability and reduced efflux ratios (e.g. compound 10 vs compound 8).

RESULTS

X-ray structure of compound 6

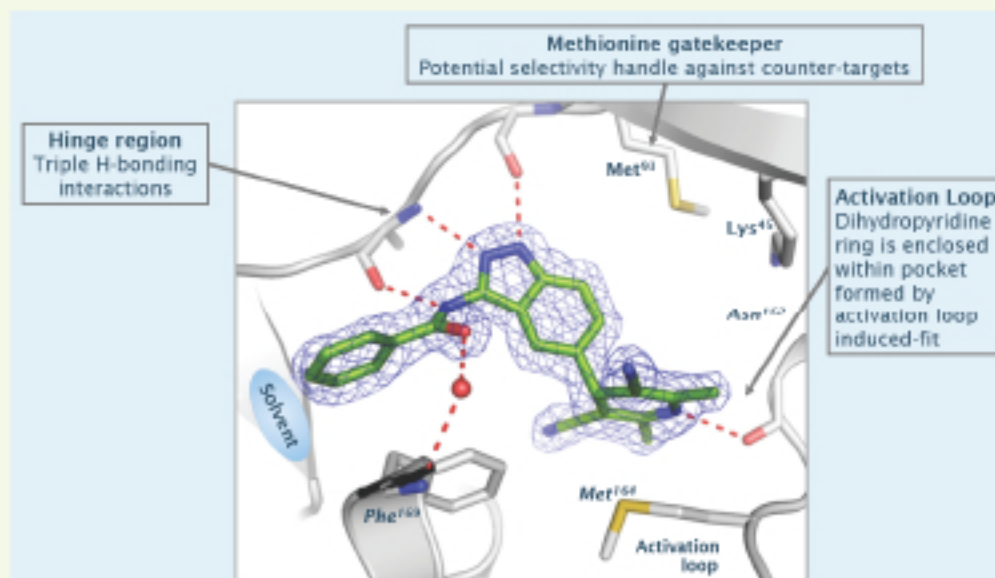


Figure 3. X-ray structure of compound 6. Only selected residues that form critical contacts with the compound are shown. Hydrogen bonds are depicted as dashed red lines. The complex structure was determined at 1.8 Å resolution.

- The X-ray structure of compound 6 in complex with the AMPKα2 domain allowed a better understanding of the binding mode (Fig. 3).

Rationale for potency improvement upon F-substitution

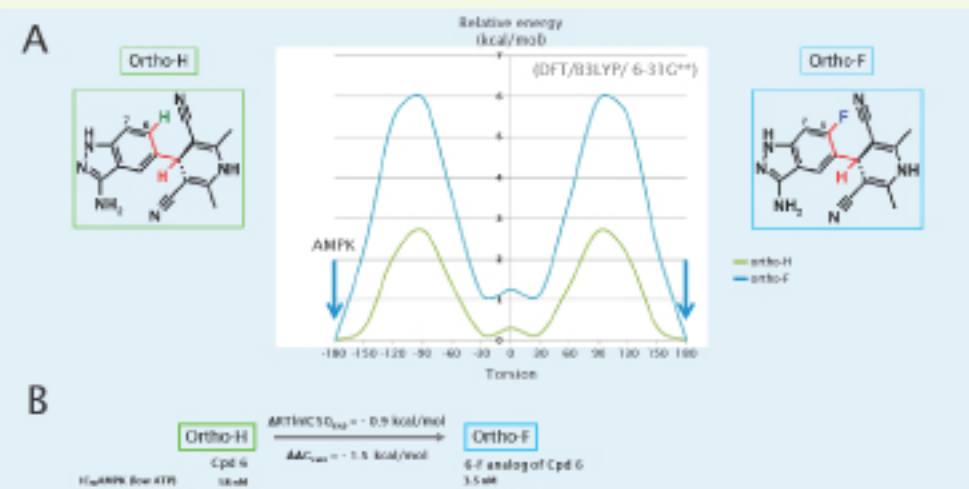


Figure 4. Rationale for potency improvement upon F-substitution. (A) Conformational analysis using ab initio quantum mechanics calculations, level of theory: (DFT/B3LYP/6-31G**). (B) FEP (free energy perturbation) calculations (software: FEP/REST, Schrödinger Inc.) utilizing X-ray of Fig. 3 to calculate free energy gain $\Delta\Delta G$ for 6-F analog of compound 6 compared to compound 6.

- Conformational analysis (Fig. 4A)
 - Trans-conformation of the core and dihydropyridine (DHP) (H-H torsion = 180°) was observed in AMPK X-ray.
 - The 6-F core (blue line) featured a much sharper and steeper energy minimum of the trans-conformation (H-F torsion = 180°) than the unsubstituted G-H core (green line).
 - Ortho-F compounds showed higher potency compared with ortho-H compounds. This may be explained by entropic reasons, as the higher energy barrier in the ortho-F compounds locks the compounds in the right AMPK-bound conformation.
- Calculation of binding free energy (free energy perturbation, FEP) (Fig. 4B)
 - Potency improvement upon F-substitution could be calculated with good accuracy.

Potency and selectivity optimization of the DHP lead structure

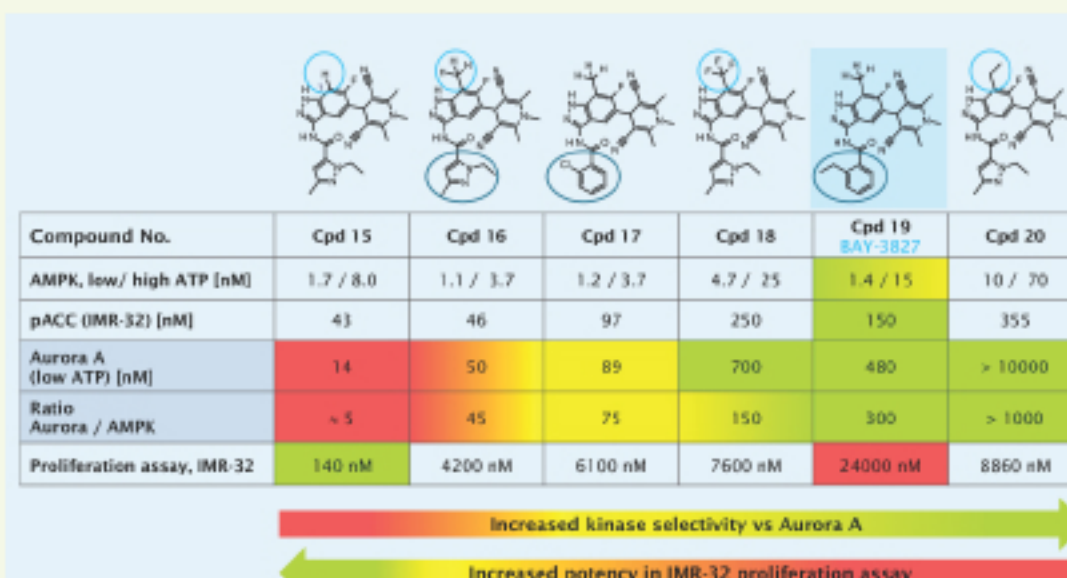


Figure 5. Chemical optimization of the DHP lead structure with respect to potency and selectivity. Structure-activity relationship analysis for modifications at C7 of the DHP core and for modifications of the amide moiety. IC₅₀ values were determined with AMPK kinase assays, with a low ATP Aurora A kinase assay, with a cellular mechanistic assay measuring phosphorylated acetyl-CoA carboxylase (pACC) and with a proliferation assay using IMR-32 neuroblastoma cells. Cpd, compound.

- The substituent at C7 of the DHP core increased the selectivity of the compounds towards Aurora kinase in the following order: -H < -Me < -CF₃ < Et (Fig. 5).
- The increased kinase selectivity of the compounds was associated with decreased potency in a proliferation assay using MYC-dependent IMR-32 neuroblastoma cells.
- Based on the high potency against AMPK and good kinase selectivity, compound 19 (called BAY-3827) was selected as a tool compound for further studies.

Potent inhibition of AMPK kinase activity does not translate into anti-proliferative activity on MYC-dependent cells *in vitro*

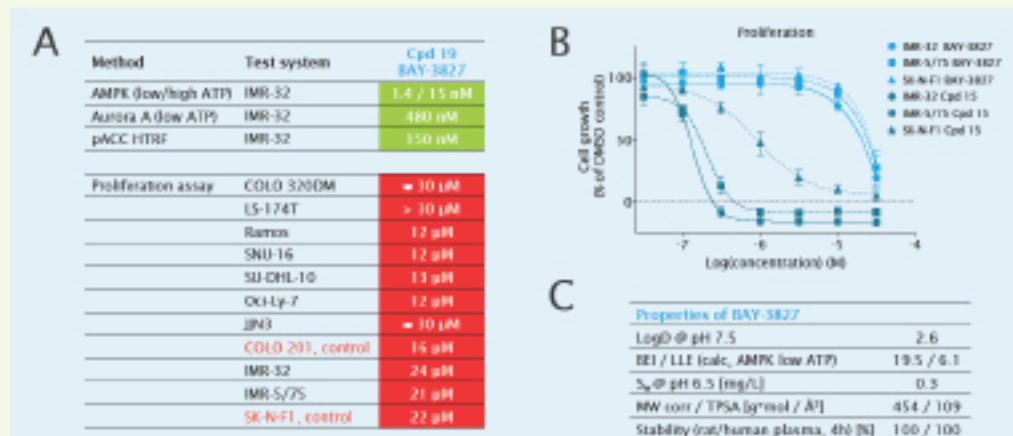


Figure 6. Effect of the AMPK inhibitor BAY-3827 on the proliferation of MYC-dependent cells. (A) The anti-proliferative effect of BAY-3827 was evaluated in a panel of cancer cell lines with dysregulated MYC signaling. The Colo201 and SK-N-F1 cell lines with no MYC dysregulation were used as control. IC₅₀ values (μM) represent mean values determined from 2-6 individual experiments. Green/red color indicates expected/unexpected results. (B) The effect of BAY-3827 and compound 15 on the proliferation of different cell lines. (C) Selected physico-chemical and calculated properties of BAY-3827. Cpd, compound; MW, molecular weight; pACC, phosphorylated acetyl-CoA carboxylase; LogD@ pH 7.5, distribution coefficient between octanol and water at pH 7.5; BE1, binding efficiency (pIC₅₀ * 1000/MW_{calc}); LLE, ligand-lipophilicity efficiency (pIC₅₀ - cLogD@ pH 7.5); Sw, solubility in water; TPSA, topological polar surface area.

- The potent and selective AMPK inhibitor BAY-3827 did not inhibit cell proliferation in cancer cell lines with dysregulated MYC signaling (Fig. 6A-B).
- BAY-3827 was found to exhibit drug-like properties (Fig. 6C).

CONCLUSIONS

- A potent and selective AMPK inhibitor, BAY-3827 (Fig. 7), was identified through high-throughput screening and subsequent chemical optimization.
- BAY-3827-induced inhibition of AMPK did not translate into anti-proliferative activity in the various tested MYC-dependent cell lines, which is in contrast to our target validation with siRNA, and might reflect activation of alternative pathways for ATP generation.
- While the initial hypothesis of this study could not be confirmed, it can be speculated that inhibition of AMPK may have therapeutic usefulness in other biological contexts.
- The availability of potent and selective inhibitors, such as BAY-3827, may nonetheless contribute to the better understanding of the biological role of AMPK signaling in cancer.

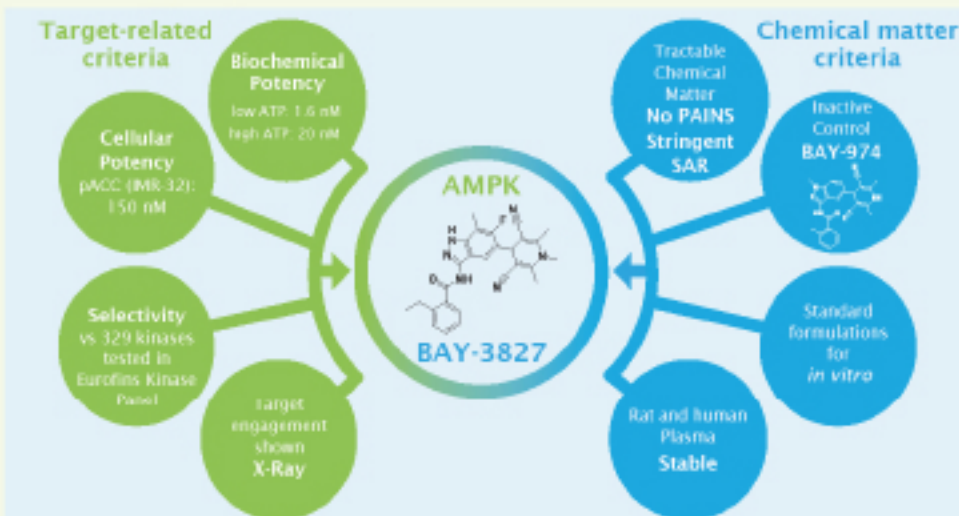


Figure 7. AMPK-Inhibitor Probe BAY-3827.

METHODS

- AMPK kinase assays were performed at both low (10 μM) and high (2 mM) ATP concentrations. Aurora A kinase assays were performed at low ATP concentrations (10 μM).
- The cellular mechanistic assay was performed in IMR-32 neuroblastoma cells using a commercially available phospho-ACC HTRF® kit (Cisbio). This assay was used to determine the level of ACC phosphorylated at Ser79 (pACC) in cell lysates.
- Caco-2 permeability was determined with an assay using Caco-2 cells purchased from DSMZ (Germany). Permeability (Papp) was measured in the apical to basolateral (A→B) and basolateral to apical (B→A) directions. The basolateral (B) to apical (A) efflux ratio was calculated using the formula Papp (B→A) / Papp (A→B).
- Proliferation assays were performed in a panel of cells with dysregulated C-MYC (COLO 320DM, LS-174T, Ramos, SNU-16, SU-DHL-10, OCI-LY7 and JIN-3) or N-MYC (IMR-32 and IMR-5/75). Colo201 and SK-N-F1 were used as control cell lines (without C-MYC/N-MYC dysregulation).

REFERENCES

- Faubert B et al., *Cancer Lett.* 2015;356:165-70.
- Jeon SM, Hay N, *Arch Pharm Res.* 2015;38:346-57.
- Liu L et al., *Nature.* 2012;483:608-12.

ACKNOWLEDGEMENTS

We thank Prof. Martin Eilers for scientific advice. Support on chemical syntheses by Pharmaron is gratefully acknowledged. Aurexel Life Sciences Ltd. (www.aurexel.com) is thanked for editorial assistance in the preparation of this poster, funded by Bayer AG.

